Award Number: W81XWH-11-1-0388

TITLE: Viral Oncolytic Therapeutics for Neoplastic Meningitis

PRINCIPAL INVESTIGATOR: Dr. Kumudu Darshini Kuruppu

CONTRACTING ORGANIZATION: Massachusetts General Hospital
Boston, MA 02114-2621

REPORT DATE: September 2014

TYPE OF REPORT: Final

PREPARED FOR: U.S. Army Medical Research and Materiel Command
Fort Detrick, Maryland 21702-5012

REPORT DOCUMENTATION PAGE

Form Approved
OMB No. 0704-0188

1. REPORT DATE	**2. REPORT TYPE**	**3. DATES COVERED**
September 2014	Final	01 July 2011 - 30 June 2014

4. TITLE AND SUBTITLE
Viral Oncolytic Therapeutics for Neoplastic Meningitis

5a. CONTRACT NUMBER
W81XWH-11-1-0388

5b. GRANT NUMBER

5c. PROGRAM ELEMENT NUMBER

6. AUTHOR(S)
Kumudu Darshini Kuruppu

E-Mail: dkuruppu@partners.org

5d. PROJECT NUMBER

5e. TASK NUMBER

5f. WORK UNIT NUMBER

7. PERFORMING ORGANIZATION NAME(S) AND ADDRESS(ES)

Massachusetts General Hospital
RICHARD BRINGHURST, M.D.
55 FRUIT ST
BOSTON MA 02114-2621

8. PERFORMING ORGANIZATION REPORT NUMBER

9. SPONSORING / MONITORING AGENCY NAME(S) AND ADDRESS(ES)
U.S. Army Medical Research and Materiel Command
Fort Detrick, Maryland 21702-5012

10. SPONSOR/MONITOR'S ACRONYM(S)

11. SPONSOR/MONITOR'S REPORT NUMBER(S)

12. DISTRIBUTION / AVAILABILITY STATEMENT
Approved for Public Release; Distribution Unlimited

13. SUPPLEMENTARY NOTES

14. ABSTRACT
Neoplastic meningitis is a fatal complication of breast cancer for which there is no cure. The project aimed to develop a novel, safe and efficient therapy for neoplastic meningitis, that of HSV-1 oncolysis. During the 1st year of the grant we prepared virus titers ($1x10^7$, $1x10^8$ and $1x10^9$ pfu/ml) for studying fractionated virus particles and developed stable breast cancer cell lines together with those that express bioluminescence (Rluc) and fluorescence (mCherry) markers for in vivo molecular imaging and tested their sensitivity to the HSV-1 oncolysis. These results were published in Cancer Research (PMC4147034; 2014). We selected MDA-MB-23-Rluc-mCherry to develop a mouse model of meningeal metastases during the 2nd year of the grant while waiting for the MGH animal facilities to be set up for housing. We characterized tumor growth in this model with sequential bioluminescence and MRI. Tumor growth occurred in 3 phases; a lag, exponential and plateau phase and was comparable with disease progression in humans. The model was presented at the annual meeting of the Society of nuclear medicine and molecular imaging (SNMMI) in Vancouver (June, 2013). The manuscript is ready for submission to Cancer Research. In the 3rd year we used this model to investigate the potential therapeutic effect of HSV-1 on meningeal metastases. When HSV-1 was injected at the early growth phase (day 12) we observed a significant reduction in tumor growth compared to the non-treated mice. Data gathered from this investigation was used to study virus distribution in the brain in the rat model. The therapeutic effect of HSV-1 oncolysis on meningeal metastases was presented (oral) at the annual meeting of the World Molecular Imaging Society (Korea, June 20114). The funding received by this award has been invaluable in terms of developing a model of neoplastic meningitis in mice and investigating the potential therapeutic effect of HSV-1 oncolysis on neoplastic meningitis. Successful data accomplished from this award has resulted in the award of an NIH R21 to further investigate HSV-1 oncolysis on meningeal metastases with molecular MRI and PET imaging (1R21CA186054-01).

15. SUBJECT TERMS
Neoplastic meningitis, mouse model, breast cancer, bioluminescence, MRI, viral oncolysis, HSV-1.

16. SECURITY CLASSIFICATION OF:			**17. LIMITATION OF ABSTRACT**	**18. NUMBER OF PAGES**	**19a. NAME OF RESPONSIBLE PERSON**
a. REPORT	**b. ABSTRACT**	**c. THIS PAGE**			USAMRMC
U	U	U	UU	28	**19b. TELEPHONE NUMBER** *(include area code)*

Progress Report -Final: 01 July 2011 - 30 June 2014

1. Introduction:

Meningeal metastasis, also known as carcinomatous meningitis is a fatal complication of breast cancer. It results when cancer cells enter the subarachnoid space and seed in the meninges. About 5% of breast cancer patients with late stage disease are diagnosed with meningeal metastases. The incidence is higher, approximately 20% when autopsy results of patients who have succumbed to systemic disease are included. Seeding of cancer cells in the meninges, arachnoid and the pia mater and their subsequent growth results in severe neurological complications that include abnormalities in cranial nerve functions (muscular and facial), cerebral symptoms (speech disturbances), and spinal cord symptoms (limb weakness), contributing to a life expectancy of 1 to 4 months. Treatment at present is largely palliative. Although aggressive multimodal therapies such as radiation, chemotherapy (intra-CSF and systemic) are attempted they are accompanied with toxicities and complications. Besides, chemotherapy is often cleared by the CSF. The secure guarding of the subarachnoid space by the blood-brain- barrier on one side and the blood-CSF barrier on the other offers less opportunity for chemotherapy to reach the cancer cells that reside within the meninges. Thus there is an urgent need for a new therapeutic modality to target meningeal metastases. Oncolytic, replication conditional HSV-1 is suggested as a therapeutic option for meningeal metastases.

We present significant findings and results obtained during the entire funding period. This includes work that has been completed during the 1st and 2nd years if the funding period and the period of no cost extension (3rd year). We propagated virus and performed plaque assays for titers required for the partnering PI's SOW towards the grant. With the additional time that remained we established and characterized a mouse model of meningeal metastases. This model served as a platform for the work proposed in the rat model in the grant. We also investigated the therapeutic effect of oncolytic HSV-1 on the mouse model. We present the study of the animal model of meningeal metastases preliminary data on effective tumor inhibition by HSV-1 oncolysis in the mouse model.

2. Keywords

Meningeal metastases, HSV-1 oncolysis, mouse model, virus replication and kinetics, cell proliferation kinetics, bioluminescence, MRI, PET.

3. Overall Project Summary:

SOW performed:
Year 1: Based on the statement of work we maintained and propagated virus, determined virus titers for the studies in the rat model of neoplastic meningitis. We also achieved the following:

1. Prepare virus and burst assays
2. Perform plaque assays for estimation of virus titer
3. Develop cell lines for future use in bioluminescent and fluorescent imaging
4. Determine the sensitivity of the cell lines to HSV-1 oncolysis.

Year 2: Based on the statement of work we studied the kinetics of virus replication (to determine the virus titer and timing of delivery) with non-invasive imaging. This data was used to determine virus titers and time of delivery in the rat model of neoplastic meningitis. The growth kinetics of the different cell lines was studied with non-invasive imaging. In addition, using one of the cell lines we developed a mouse model of meningeal metastases. Our achievements include the following:

1. Studied the kinetics of virus replication in vivo.
2. Studied the kinetics of cancer cell proliferation and their response to viral oncolysis in vivo.

The results are published in Cancer Research (Appendix A).

3. Established a mouse model of meningeal metastases (Neoplastic meningitis) with molecular imaging.

The characterization of the model was presented as a poster presentation at SNMMI 2014 (Appendix B)

Year 3: The mouse model of meningeal metastases was further characterized to correlate in vivo imaging data with in vitro immunohistochemical staining data. Observations from this model were relevant to determine locations of metastases and their growth when optimizing the rat model. Our achievements include the following:

1. Characterized the mouse model of meningeal metastases (Neoplastic meningitis) with molecular imaging correlating with histology.

A manuscript is being submitted for publication to Cancer Research.

2. Investigated the therapeutic effect of HSV-1 oncolysis for meningeal metastases in the model.

The model was created in nude mice using the stably transfected human MDA-MB-231-Rluc breast cancer cells that expresses renilla luciferase (Rluc). The cells ($2x10^4$ cells in 10µl) were injected into the right lateral ventricle of the mouse brain by stereotactic coordinates. The course of tumor development in the meninges and brain compartments were studied over successive time points over 3 weeks with MRI, Rluc bioluminescence and histology (Fig 1A). Disease manifestation was observed with physical parameters such as weight, movement, and behavior.

The potential therapeutic effect of HSV-1 oncolysis was studied in this model. Virus was injected into the right lateral ventricle 14 days after tumor induction. Tumor response was studied with MRI and the observations were correlated with histology of brain sections (Fig 1B). The observations from our preliminary investigations are significant and encouraging for future treatment of meningeal metastases as currently there is no hope for a cure. Treatment of meningeal metastases with oncolytic HSV-1 is novel. These observations require further investigation of this therapeutic modality in this model.

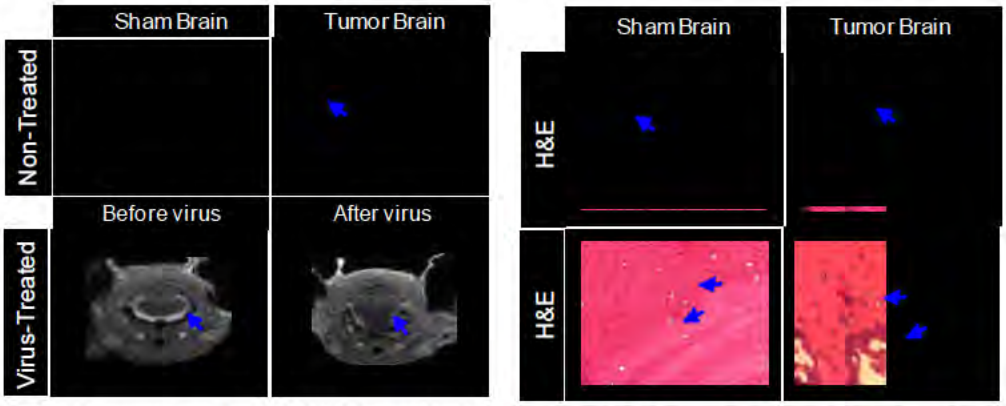

Fig 1: Therapeutic effect of HSV-1 oncolysis studied with MRI correlated with histology. Fig 1A: Gd-MRI scans show enhanced uptake of contrast agent in the meninges (arrow) in the tumor brain compared to the sham brain. In the virus treated mice the enhanced contrast uptake seen before virus injection (arrow) is diminished significantly after virus injection. Fig 1B: H&E stained histological sections show highly proliferative tumor band in the meningeal layer (arrow) in the tumor brain compared to the sham brain. Tumor is also seen around the blood vessels (arrows) in the tumor brain and absent in the sham brain.

4. Key Research Accomplishments:

We obtained the following key accomplishments:

1. Generated breast cancer cell lines and studied their sensitivity to HSV-1 oncolysis
2. Established a mouse model of meningeal metastases
3. Characterized the model with sequential imaging, histology to confirm its clinical relevance
4. Investigated the therapeutic potential of oncolytic HSV-1 to demonstrate a market inhibition of tumor growth.
5. Generated preliminary data to sustain funding to perform imaging studies on the existing model.
6. Prepared virus and derived data relevant for the rat model study of my Co-investigator.

5. Conclusion

We have performed the relevant studies on viral kinetics and responses by breast cancer cell lines to oncolytic virus replication as outlined in the statement of work. In addition, we have established a mouse model of meningeal metastases and characterized it in terms of tumor growth and external characteristics using MRI, histology, body weight and pathological symptoms. The data obtained served as a platform for studying virus distribution in the rat model described in the statement of work. We further investigated the potential therapeutic effect of HSV-1 oncolysis in the newly established mouse model with encouraging results.

6. Publications, Abstracts, and Presentations

Presentations & Abstracts:

1. Oral Presentation at WMIC, Seoul.
"Novel oncolytic HSV-1 therapeutics for breast cancer meningeal metastases"
Darshini Kuruppu, Deepak Bhere, Chris Farrar, Anna-Liisa Brownell, Umar Mahmood, Kenneth Tanabe World Molecular Imaging Congress (WMIC), Seoul, June 2014.

2. Poster Presentation at SNMMI, Vancouver.
Characterization of the animal model was presented at the annual meeting of the Society of nuclear medicine and molecular imaging, Vancouver, June 2013.

Publications:

1. Molecular imaging with bioluminescence and PET reveals viral oncolysis kinetics and tumor viability.
Kuruppu D, Brownell AL, Shah K, Mahmood U, Tanabe KK. (PMID:24876106)
Cancer Res. 2014 Aug 1;74(15):4111-21. doi: 10.1158/0008-5472.CAN-13-3472. Epub 2014 May 29.

2. Pending Manuscript:
A model of meningeal metastases from breast cancer: molecular characterization with MRI.
Kuruppu D, Bhere D, Farrar C, Shah K, Mahmood U, Tanabe KK.

7. Inventions, Patents and Licenses

In the process of discussing with the Institutions licensing office to determine eligibility for patenting the mouse model of meningeal metastases.

8. Reportable Outcomes

We have developed and presented a well characterized and clinically relevant animal model of meningeal metastases. This model is of significance with clinical relevance due to 3 key features: (i) tumor cell dissemination occurs via the cerebrospinal fluid once the cells are injected into the subarachnoid space following the route of cancer cell dissemination in the humans disease condition; (ii) the progression of meningeal metastases occurs similar to the human disease condition with tumor load in the base of the brain expressing clinical symptoms of irreversible damage resulting in central nervous system (CNS) nerve involvement; (iii) this is a model that has been fully characterized in terms of tumor progression with sequential molecular imaging over time and accompanying histological, pathophysiological and behavioral data.

The potential therapeutic effect of HSV-1 oncolysis for meningeal metastases that was investigated in this model is promising. When HSV-1 was injected into the cerebrospinal fluid (CSF) at the intermediate stage of disease progression we observed a marked reduction in tumor growth and in the progression of life threatening clinical symptoms.

9. Other Achievements

Grants Awarded:
Received an NIH-R21 based on the initial research data on the mouse model that was generated.
Fund: Novel oncolytic HSV-1 therapy for breast cancer meningeal metastases
Role: Principal Investigator
Sponsor: NIH
Award No: 1R21CA186054-01

10. References

1. Kuruppu D, Brownell AL, Shah K, Mahmood U, Tanabe KK. Molecular imaging with bioluminescence and PET reveals viral oncolysis kinetics and tumor viability. Cancer Res. 2014 Aug 1;74(15):4111-21.
2. Kuruppu D, Brownell A, Zhu A, Yu M, Wang X, Kulu Y, Fuchs B, Kawasaki H, Tanabe KK. Positron emission tomography of herpes simplex virus 1 oncolysis. Cancer Research. 2007; 67(7): 3295.
3. Kuruppu D, Tanabe KK. Viral oncolysis by herpes simplex virus and other viruses. Cancer Biology & Therapy. 2005; 4(5): 524-31.

11. Appendices

A. Cancer Research Publication
B. SNMMI poster presentation
C. WMIC oral presentation
D. SNMMI Abstract
E. WMIC Abstract

Appendix A: Cancer Research Publication

Published OnlineFirst May 29, 2014; DOI: 10.1158/0008-5472.CAN-13-3472

Cancer Research

Molecular Imaging with Bioluminescence and PET Reveals Viral Oncolysis Kinetics and Tumor Viability

Darshini Kuruppu[1], Anna-Liisa Brownell[2], Khalid Shah[2], Umar Mahmood[2], and Kenneth K. Tanabe[1]

Abstract

Viral oncolysis, the destruction of cancer cells by replicating virus, is an experimental cancer therapy that continues to be explored. The treatment paradigm for this therapy involves successive waves of lytic replication in cancer cells. At present, monitoring viral titer at sites of replication requires biopsy. However, repeat serial biopsies are not practically feasible for temporal monitoring of viral replication and tumor response in patients. Molecular imaging provides a noninvasive method to identify intracellular viral gene expression in real time. We imaged viral oncolysis and tumor response to oncolysis sequentially with bioluminescence and positron emission tomography (PET), revealing the kinetics of both processes in tumor xenografts. We demonstrate that virus replication cycles can be identified as successive waves of reporter expression that occur ~2 days after the initial viral tumor infection peak. These waves correspond to virions that are released following a replication cycle. The viral and cellular kinetics were imaged with Fluc and Rluc bioluminescence reporters plus two 18F labeled PET reporters FHBG [9 (4 18F fluoro 3 [hydroxymethyl] butyl) guanine] and FLT (18F 3′ deoxy 3 ′fluorothymidine), respectively. Correlative immunohistochemistry on tumor xenograft sections confirmed *in vivo* results. Our findings show how PET can be used to identify virus replication cycles and for real time measurements of intratumoral replicating virus levels. This noninvasive imaging approach has potential utility for monitoring viral oncolysis therapy in patients. *Cancer Res; 74(15); 4111 21. ©2014 AACR.*

Introduction

Viral oncolysis by Herpes Simplex virus 1 (HSV 1) is cur rently being investigated for cancers unresponsive to conven tional treatment. Replication conditional HSV 1 mutants are genetically engineered for effective oncolysis. These mutants replicate preferentially in cancer cells rather than in normal cells, which forms basis for safety and efficacy of this approach (1, 2). The process of oncolysis begins when the virus infects a tumor cell. Progeny virions that are liberated at the end of a replication cycle infect neighboring cancer cells to begin another wave of replication. The process continues until the cancer is eliminated or the virus is extinguished by the host defense mechanisms. Thus, the initially injected virus titer is amplified to a larger virus titer to destroy the cancer cells (3, 4). HSV 1 is among several oncolytic viruses that are studied, which include reovirus, vaccinia virus, poxvirus, adenovirus, and vesiculostomatitis virus (5 8). HSV 1 has an advantage over some of the other oncolytic viruses because of its large genome capacity, nonintegration of its DNA into the host genome, and high infectivity in cancer cells. The availability of antiherpetic drugs such as acyclovir and gancyclovir provide added safety as they can help terminate unwanted viral rep lication if needed (9 11).

Monitoring is needed during viral oncolysis therapy to identify virus titer at sites of virus replication. The current method of biopsy is not feasible for repetitive virus assessment. The absence of a reliable and clinically applicable method to measure viral activity in real time is a major drawback for monitoring viral oncolysis therapy in clinical trials. The non invasive and dynamic imaging capabilities of bioluminescence and positron emission tomography (PET) provide a means to image viral replication repetitively *in vivo*, preclinically for bioluminescence and both preclinically and for clinical trans lation with PET. Using specific reporters for each imaging modality, the kinetics of virus replication can be studied by identifying sites and intensity of reporter expression. In addi tion, the destruction of cancer cells undergoing viral oncolysis can be simultaneously studied.

Bioluminescence imaging provides rapid, short interval, serial imaging for kinetic studies. Because of its high target to background ratio, bioluminescence offers a sensitive and robust tool for studying gene expression and function (12 14). Through multireporter imaging of distinct sub strates, temporal relationships between multiple biological processes and their pathological manifestations in cancer, artherosclerosis, and neurological disorders, and treatment response can be defined (15 18). The kinetics of virus replication and the tumor response to lytic replication can be simultaneously studied *in vivo*, in preclinical models using this approach.

Authors' Affiliations: Departments of [1]Surgery and [2]Radiology, Massa chusetts General Hospital, Boston, Massachusetts

Corresponding Author: Kenneth K. Tanabe, Massachusetts General Hospital, 55 Fruit Street, Boston, MA 02114.

doi: 10.1158/0008 5472.CAN 13 3472

Published OnlineFirst May 29, 2014; DOI: 10.1158/0008-5472.CAN-13-3472

In contrast, PET is readily translatable to human studies. It is routinely used with [^{18}F]FDG as a sensitive noninvasive imaging method to identify and stage tumors, determine treatment success and disease recurrence at the deep tissue level without background tissue interference. The prototype enzyme reporter, HSV thymidine kinase (TK) is ideal for imaging virus replication in tumors with PET. Based on the promiscuity of HSV TK, the guanine derivative 9 [3 fluoro 1 hydroxy 2 propoxymethyl] guanine (FHBG; refs. 19 and 20) serves as a substrate for viral TK. The phosphorylated [F18 labeled] FHBG, which is trapped inside cells is detected with PET. We have previously reported that HSV 1 oncolysis can be imaged with PET using FHBG as the substrate for HSV TK (21). However, because of the large viral titer used in the study, PET imaging was restricted to the early stages of virus replication. Imaging beyond this stage was not possible because most of the cancer cells were destroyed. The kinetics of virus replication can be better understood by sequential study of oncolysis. To address this in a more clinically relevant scenario, we assessed lower titers and used the replication conditional oncolytic HSV 1 mutants, hrR3 and HSV Luc. Because of LacZ gene insertion into the gene locus for viral ribonucleotide reductase, these mutants replicate preferentially in cancer cells where the abundant nucleotides substitute for the absent ribonucleotide reductase gene product (22, 23). HSV Luc in addition expresses the Fluc gene.

Here we present our investigations on the kinetics of HSV 1 replication and the accompanying tumor response to oncolysis with dual bioluminescence and PET imaging. Through optimization of dose, dosing intervals, and substrate for reporters, we identify, for the first time, virus replication cycles as waves in bioluminescence and PET reporter expression. In addition, by studying the kinetics of tumor cells subjected to oncolysis we show a reduction in tumor burden subsequent to lytic replication. These results support the translatability of monitoring virus replication with serial PET scans using [^{18}F]FHBG.

Materials and Methods

Development of stable cell lines for bioluminescence imaging

Human cancer cell lines [MDA MB 231 breast cancer (ATCC HTB 26), A2058 amelanotic melanoma (ATCC CRL 11147), and HT29 colon cancer (ATCC HTB 38)] and mouse cancer cell lines [4T1 breast cancer (ATCC CRL 2539) and MC26 colon cancer] were engineered to express Rluc. The human cell lines were maintained in RPMI 1640 medium supplemented with 10% FBS, whereas the murine cell lines were maintained in DMEM supplemented with 10% FBS. The cell lines were obtained from ATCC and were used in this study for less than 6 months after resuscitation. They are authenticated by ATCC after a comprehensive quality control before shipment. MC26 was kindly provided by Dr. R.L. Martuza. The cell lines were tested for mycoplasma, Hoechst DNA staining, PCR, and culture testing for contaminant bacteria, yeast, and fungi. Authentication procedures used include species verification by DNA bar coding and identity verification by DNA profiling.

The cell lines were infected with lentivirus containing cDNA for Rluc and mCherry as well as puromycin resistance. Within 18 to 24 hours after infection, approximately 90% of cells expressed mCherry fluorescence. These cells were detached with trypsin and plated in 6 well dishes in media containing puromycin (10 μg/mL). This allowed growth of cells with the newly incorporated lentivirus DNA containing the mCherry, Rluc, and the puromycin resistance gene. Over the following week, colonies that developed in media containing puromycin were examined for mCherry expression under an inverted phase contrast fluorescence microscope. The colony that expresses the strongest mCherry signal for each of the cell lines was expanded for our experiment. The Rluc expression was validated with coelenterazine.

Replication conditional HSV 1 mutants

The replication conditional HSV 1 mutant that expresses Fluc (HSV Luc) was generated by a bacterial artificial chromosome (BAC) based HSV cloning system (kindly provided by Dr. R.L. Martuza) utilizing Flip Flop HSV BAC technology (23). The HSV Luc contains the luciferase expression cassette driven by the cytomegalovirus (CMV) promoter and the LacZ gene inserted in the middle of the UL39 (ICP6) gene. The replication conditional HSV 1 mutant hrR3 has the ICP6 inactivated by insertion of the LacZ gene (22). The viruses were propagated in Vero cells and replication assays were performed to determine the titer as previously described (24).

In vitro measurement of virus with Fluc bioluminescence

Cancer cells (MDA MB 231 and MC26) were plated in 24 well plates at a concentration of 6×10^4 cells/well. A day later, the cells were exposed to different titers of HSV Luc [1×10^3 to 1×10^8 plaque forming units (pfu)]. The virus was imaged with bioluminescence using luciferin. To determine the kinetics of virus replication, Fluc expression was imaged over sequential time points at 6, 12, 18, 24, 30, and 36 hours after infection. This bioluminescence signal was expressed as the net intensity per area of triplicate wells. A viable cell count was performed using trypan blue exclusion for each well. This was done at each of the time points that were imaged.

In vitro measurement of virus with TK PET

Cancer cells (MC26) and Vero cells were plated in 6 well plates at a concentration of 4×10^5 cells/well. Once the cells were 80% confluent they were infected with 1×10^8 pfu hrR3. Virus expression in the cells was determined by incubating the cells with [^{18}F]FHBG for 2 hours, followed by 2 washes. The [^{18}F]FHBG uptake by the cells was measured by a γ counter (Packard Cobra 5005), and was expressed per cell. The concentration of cells in each well was determined by a viable cell count.

Flank tumor model

BALB/c nude mice were obtained from the COX institutional animal breeding services (Steele Laboratories). All experiments were performed according to the institutional subcommittee on research animal care. The mice were housed in an authorized animal facility with free access to food and

Published OnlineFirst May 29, 2014; DOI: 10.1158/0008-5472.CAN-13-3472

water. Flank tumors were created in mice using each of the stable cell lines that were developed and grown in culture. The cells were trypsinized and washed in medium containing serum to inactivate trypsin. After a PBS wash, the cells were prepared for injections. Each cell line was injected into groups of ten mice. 1×10^5 cells from each cell line in 100 μL PBS were injected bilaterally or to one side of the flank. Experiments were commenced when the tumors reached 5 mm in diameter.

In vivo virus and tumor imaging with dual Fluc and Rluc bioluminescence

The animals were randomized into control and virus treatment groups. Tumors in both groups were imaged for Rluc bioluminescence every other day for 8 days. Images were acquired for 10 minutes after coelenterazine injection (7.5 μg i.v./mouse) at 8 × 8 binning (Carestream Molecular Imaging). HSV Luc (1×10^8 pfu/50μL in PBS) was injected into the tumor center and imaged daily for 8 days. The virus treated group underwent dual imaging for Fluc and Rluc. Fluc bioluminescence was acquired for 10 minutes at 8 × 8 binning after luciferin injection (3.5 μg i.p./mouse). Fluc images were acquired a minimum of 6 hours after Rluc images were captured to allow for complete clearance of the Rluc signal. Each of the Rluc and Fluc images was overlaid onto an X ray image captured for 20 seconds. Tumor volume was calculated in the control and treatment groups with caliper measured tumor diameter. Bio luminescence signal was quantified using the imaging software (Carestream). Regions of interest were normalized to back ground intensity and expressed as net intensity per unit area.

In vivo virus and tumor imaging with microPET

When the bilateral flank tumors reached 5 mm in diameter, virus was injected directly into the left tumor, whereas the right tumor served as the control. The mice were positioned into the scanner under isoflurane anesthesia (1% 1.5% isoflurane with 2 L/min oxygen). We used a microPET scanner with a reso lution of 4.1 mm^3 (microPET P4; Concorde Microsystems, Inc.). Transmission images were gathered with the aid of 57Co

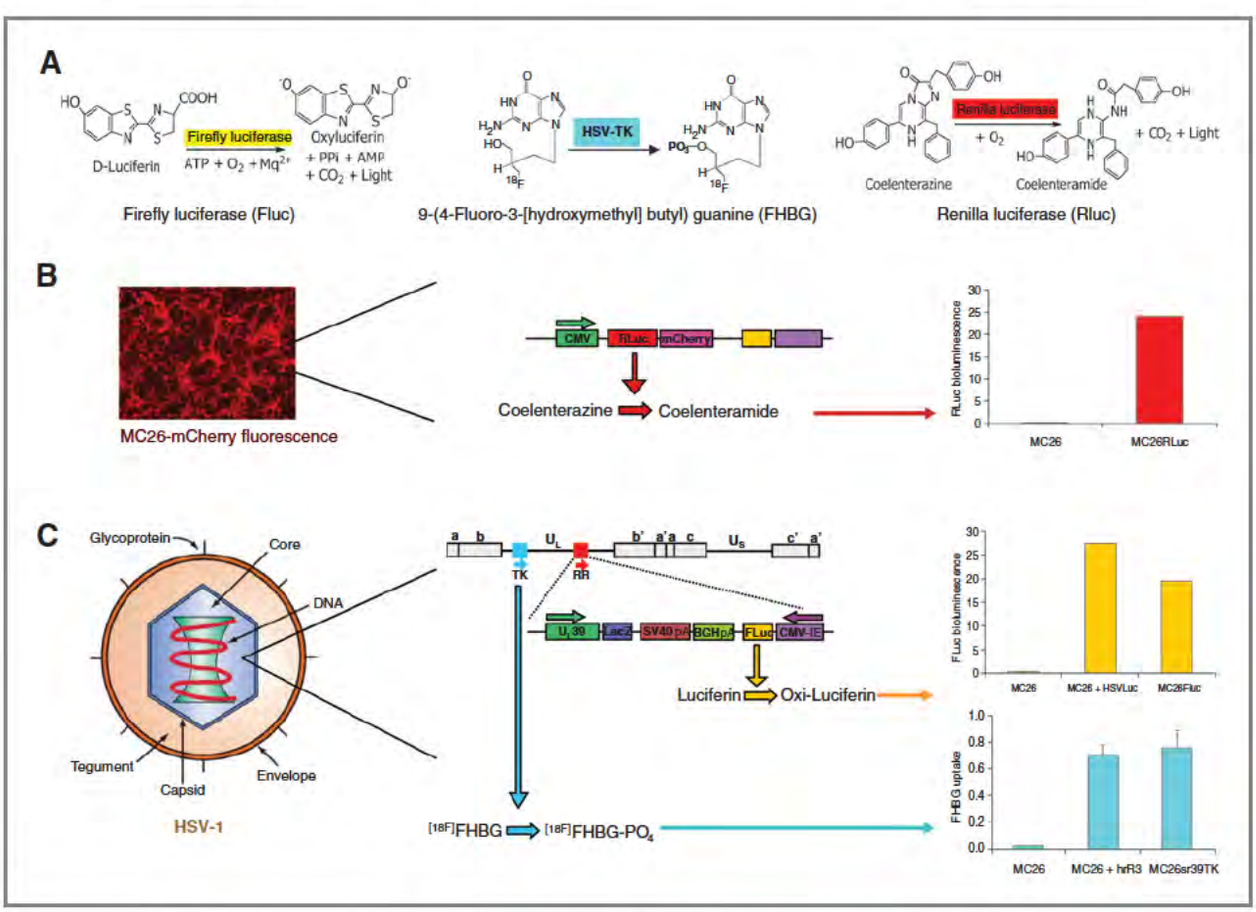

Figure 1. Schematic characterization of molecular reporters, cells, and virus. A, the dual bioluminescence detection system is based on the enzymatic reaction of Fluc and Rluc, where luciferin and coelenterazine serves as substrates. The PET ligand [^{18}F]FHBG, serves as the substrate for HSV TK, which phosphorylates and traps it intracellularly. B, stable cancer cell lines that express Rluc and mCherry can be identified with Rluc bioluminescence and mCherry fluorescence. Transformed MC26 cells imaged for Rluc *in vitro* are shown. C, HSV Luc expresses the Fluc and TK genes. The replicating virus was identified in MC26 cells with Fluc bioluminescence *in vitro* (MC26+HSV Luc), and the signal was comparable to MC26 cells that transiently express Fluc (MC26 Fluc). The virus replicating in MC26 cells was detected with the PET tracer [^{18}F]FHBG *in vitro* (MC26+hrR3). The [^{18}F]FHBG signal was comparable to that of MC26 cells, which express the TK gene transiently (MC26sr39TK).

Published OnlineFirst May 29, 2014; DOI: 10.1158/0008-5472.CAN-13-3472

to correct for attenuation. Dynamic volumetric data were obtained for 120 minutes after [^{18}F]FHBG (100 μCi t.v./mouse) injection. Volumetric images were reconstructed with filtered back projection after the data were corrected for uniformity, scatter, attenuation, decay, and injected activity using Asi Pro4.1 software. Time activity curves were generated from the selected regions of interest from the control tumor, virus injected tumor, the liver, and the heart. PET signal was expressed as the % radiolabel accumulation/injected dose/cc. Imaging studies with [^{18}F]FHBG were conducted at 2, 6, 24, 48, and 72 hours for different virus titers (hrR3 at 1×10^9, 1×10^7, 1×10^5, and 1×10^3 pfu). The background activity was measured before injecting the [^{18}F]FHBG at each time point to correct for any residual signal from the dose that preceded it. Although negligible, this measurement was corrected with the injected dose. The tumor response to lytic replication was imaged with [^{18}F]FLT PET.

Identification of virus with LacZ in frozen tumor sections

Frozen tumors were sectioned at 5 μm and mounted on superfrost coated microscope slides (Fisher Scientific). The sections were fixed in 3% glutaraldehyde before LacZ staining for β galactosidase. The sections were incubated in 5 bromo 4 chloro 3 indolyl β D galactopyranoside (X gal) solution at 37°C overnight. The X gal solution was prepared as follows: X gal at 20 mg/mL in dimethyl formamide, 0.1 M potassium ferricyanide, 0.1 M potassium ferrocyanide, and 0.1 M $MgCl_2$ (Sigma). Areas of LacZ expression appeared blue. Sections were coverslipped and studied under a light microscope.

Hematoxylin and eosin and IHC staining for HSV TK, proliferating cell nuclear antigen, and terminal deoxynucleotidyl transferase dUTP nick end labeling staining of tumors

Formalin fixed tumors were processed, paraffin embedded, and serial sections were mounted for hematoxylin and eosin (H&E), HSV TK, proliferating cell nuclear antigen (PCNA), and terminal deoxynucleotidyl transferase dUTP nick end labeling (TUNEL) staining. HSV TK IHC was performed after antigen retrieval in citrate buffer. Endogenous peroxidase and serum were blocked before HSV TK antiserum was applied at 1:5,000 dilution overnight at 4°C. The sections were incubated in

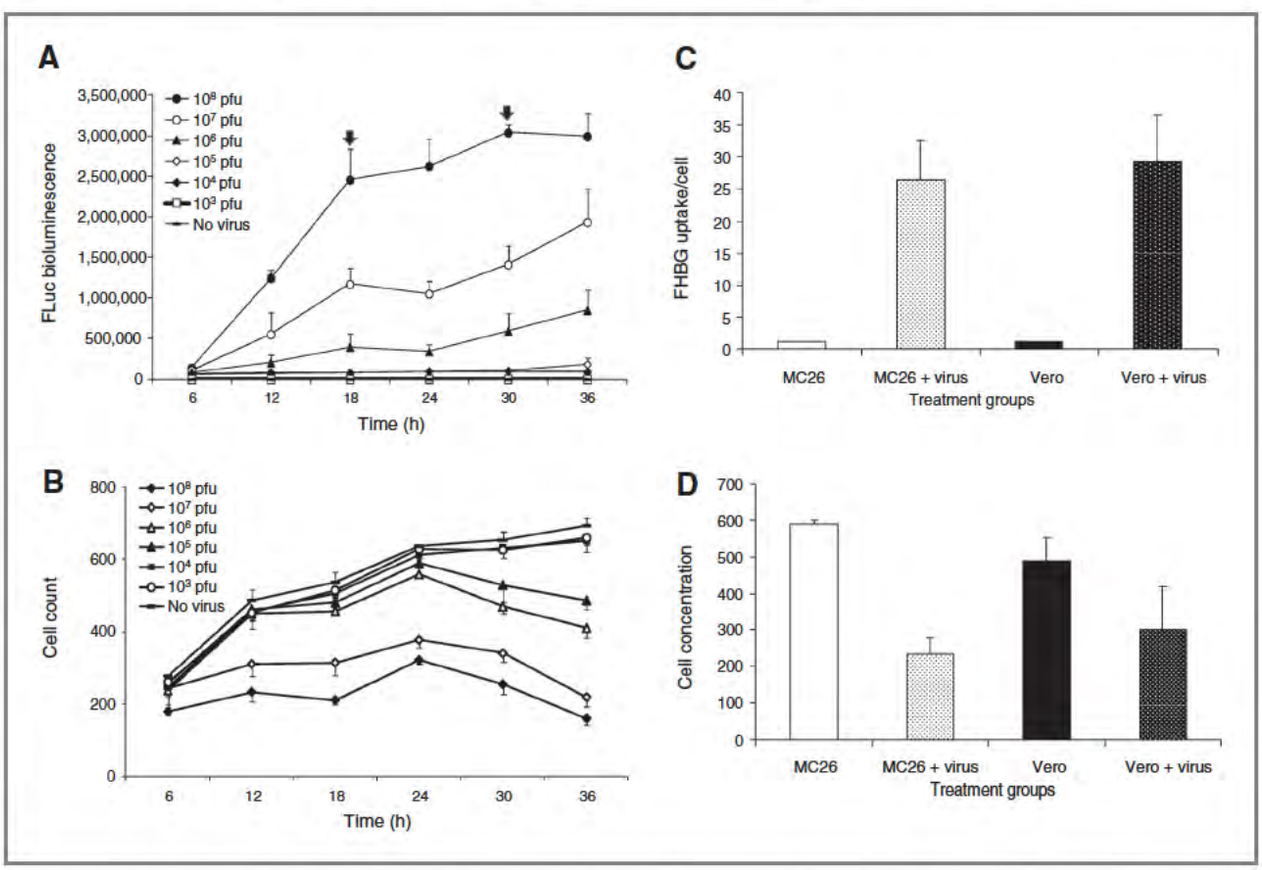

Figure 2. Kinetics of virus and cells *in vitro* determined with bioluminescence and PET substrates. A, the replication kinetics of HSV Luc in MC26 cells studied with Fluc bioluminescence. Two peaks (arrows) were observed in the Fluc signal in the high virus titers (1×10^8, 1×10^7, and 1×10^6 pfu), whereas the signal was undetectable in the lower virus titers. Fluc signal is expressed as the mean net intensity/area ± SD. B, viability of MC26 cells infected with virus. The cell counts decreased when infected with high viral titers (1×10^8, 1×10^7, and 1×10^6 pfu). Cell count is expressed as the mean ± SD. C, [^{18}F]FHBG uptake in MC26 and Vero cells 24 hours after HSV Luc (1×10^8 pfu) infection. Data are the mean% of ID of [^{18}F]FHBG uptake/cell ± SD. D, changes in MC26 and Vero cell concentration once infected with virus. The MC26 cell concentration was markedly reduced compared with cells not infected with virus. Cell concentration is expressed as the mean ± SD.

Published OnlineFirst May 29, 2014; DOI: 10.1158/0008-5472.CAN-13-3472

biotinylated goat anti rabbit secondary antibody, followed by horseradish peroxidase, before chromogen development with peroxidase substrate 3,3′ diaminobenzidine (DAB). HSV TK positive cells appeared brown. PCNA IHC was performed using the PCNA antibody (raised in mice; Millipore) overnight at 1:1,000 at 4°C. The antibody was detected with biotinylated antimouse secondary antibody as described above. PCNA positive cells appeared brown. Apoptosis staining was per formed using the ApopTag Fluorescein In Situ Apoptosis Detection Kit (Millipore), which detects DNA strand breaks by the TUNEL method. After proteinase K treatment, the sections were incubated with terminal deoxynucleotidyl transferase enzyme, followed by incubation with antidigoxigenin peroxi dase conjugate and counterstained with propidium iodide. ApopTag positive cells were detected under fluorescence.

Statistical analysis

Data were expressed as the mean ± standard deviation (SD), unless otherwise specified as the mean ± standard error of the mean (SEM)] and were compared using an unpaired 2 tailed *t* test. The *P* values were compared with the controls dataset.

Results

Stable cell lines and virus can be detected through bioluminescence and PET imaging

The cell lines (human MDA MB 231, A2058, HT29, and mouse 4T1 and MC26) stably transformed to express mCherry and Rluc were detected through red fluorescence and biolu minescence, respectively (Fig. 1B). The replication conditional HSV 1 mutant (HSV Luc), which contains the Fluc and TK genes, can be imaged with bioluminescence and PET (Fig. 1C). Virus replication in MC26 cancer cells was imaged with Fluc bioluminescence. The Fluc signal was comparable to that of MC26 cells, which stably express Fluc (Fig. 1C, top graph). Virus replication was identified with [^{18}F]FHBG PET. Radiolabel uptake in MC26 cells infected with virus was comparable to MC26 cells that stably express the mutant viral TK (MC26 sr39TK; Fig. 1C, bottom graph).

Kinetics of virus replication measured *in vitro* with bioluminescence and PET tracers

The kinetics of virus replication was studied *in vitro* with Fluc bioluminescence. The Fluc signal intensity correlated with the virus titer while it increased over time. In the highest virus titer (1×10^8 pfu HSV Luc), two peaks were identified at 18 and 30 hours after infection, which corresponded to virus replication cycles (Fig. 2A). The cell counts decreased over time suggestive of lytic replication. Low titers (1×10^3, 1×10^4, and 1×10^5 pfu) were undetectable with bioluminescence, whereas the cell counts increased over time, similar to the uninfected controls (Fig. 2B). The kinetics of virus replication (hrR3 at 1×10^8 pfu) studied *in vitro* with the PET tracer [^{18}F]FHBG demonstrated a marked radiolabel uptake in virus infected MC26 and Vero cells (Fig. 2C). This was accompanied by a reduction in cell concentration (Fig. 2D), indicative of lytic replication.

Identification of virus replication cycles *in vivo* with bioluminescence and PET imaging

The kinetics of HSV 1 replication was studied sequentially with bioluminescence and PET in mice bearing tumor xeno grafts (MDA MB 231 and MC26). Virus (HSV Luc at 1×10^9, 1×10^8, and 1×10^7 pfu) replication in MDA MB 231 tumors imaged with bioluminescence showed peaks in Fluc reporter expression over time. The intense peak at day 1 was followed by two smaller peaks at day 3 and day 5 as the signal decreased (Fig. 3A). The peaks correlated with virus released following a replication cycle, confirmed by plaque assay. Although the "wave" pattern was consistent, the signal intensity corre lated with the virus titers. Virus (hrR3 at 1×10^9, 1×10^7 1×10^5,

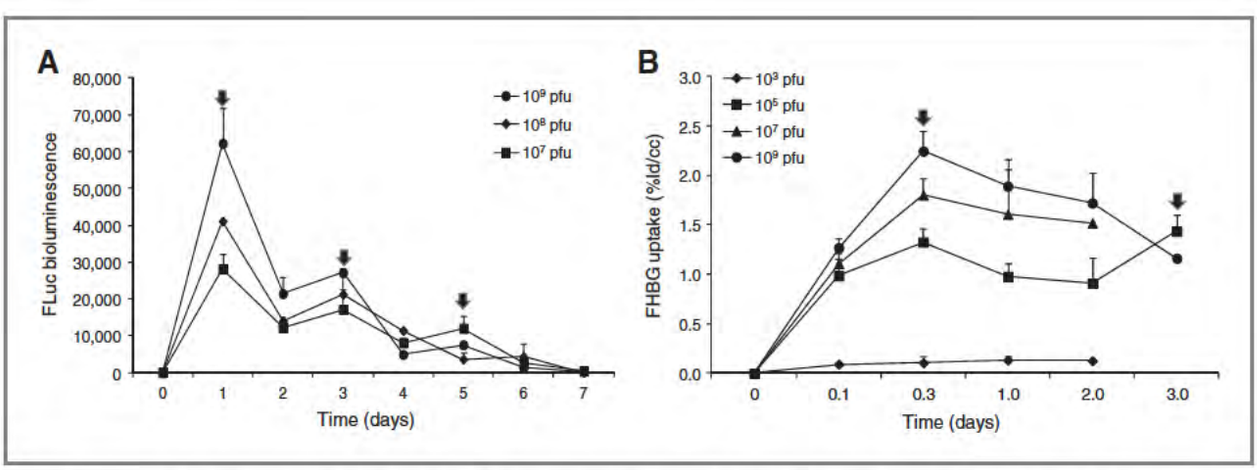

Figure 3. Dynamics of virus replication *in vivo* imaged with bioluminescence and PET. A, kinetics of virus replication in flank tumors studied with Fluc bioluminescence. The Fluc signal expressed three peaks (arrows) that decreased in intensity over time. Fluc signal is presented as the mean net intensity/area ± SD. B, kinetics of virus replication imaged with [^{18}F]FHBG PET. The [^{18}F]FHBG uptake in tumors peaked (arrows) at 6 hours (0.3 days) in the high virus titers. It decreased in highest virus titer (1×10^9 pfu), whereas it peaked again at 3 days in the lower titer (1×10^5 pfu). The lowest titer (1×10^3 pfu) had no signal. The radiolabel uptake is presented as the mean ± SD of the % injected dose/cc.

Published OnlineFirst May 29, 2014; DOI: 10.1158/0008-5472.CAN-13-3472

and 1×10^3 pfu) replication in MC26 flank tumors imaged with PET showed a profile similar to that observed with bioluminescence. The [^{18}F]FHBG reporter accumulation in cancer cells infected with 1×10^5 pfu hrR3 expressed a "wave" like pattern over 3 days. The peaks were identified at 6 hours (0.3 days) and 72 hours (3 days) and correlated with virus titers confirmed by plaque assays on tumors after imaging. The [^{18}F]FHBG signal in the highest titer (1×10^9 pfu) decreased after the initial peak at 6 hours (Fig. 3B), whereas infection with 1×10^3 pfu was undetectable.

Tumor growth kinetics identified with bioluminescence correlates with *in vitro* volumetric data

Growth kinetics of human (MDA MB 231 Rluc, A2058 Rluc, and HT29 Rluc) and mouse (4T1 Rluc and MC26 Rluc) cancer cells growing in the flanks were studied with sequential Rluc bioluminescence imaging over 8 days. Tumor volume was calculated from caliper measurements at each time point for comparison. The Rluc expression in the bioluminescence scans that defines tumor borders increased over time in all three tumor xenografts (Fig. 4A, C, and E). The calculated Rluc signal intensities for each tumor xenograft correlated with external tumor volume measured from caliper readings (Fig. 4B, D, and F). These parameters define tumor growth. We observed similar growth dynamics with bioluminescence and correlation with volumetric measurements from caliper readings in flank tumors from mouse breast cancer cells (4T1 Rluc; Supplementary Fig. S1).

Dynamics of virus replication and tumors undergoing oncolysis imaged with dual bioluminescence

The dynamics of virus replication and tumor response was studied with dual Fluc and Rluc bioluminescence following HSV Luc infection of MDA MB 231 Rluc tumors. Mice were randomized into treatment and control groups when the tumors reached 5 mm in diameter. Virus (1×10^8 pfu) was injected to the treatment group once baseline Rluc readings were obtained. Both groups were imaged over 8 days. The area

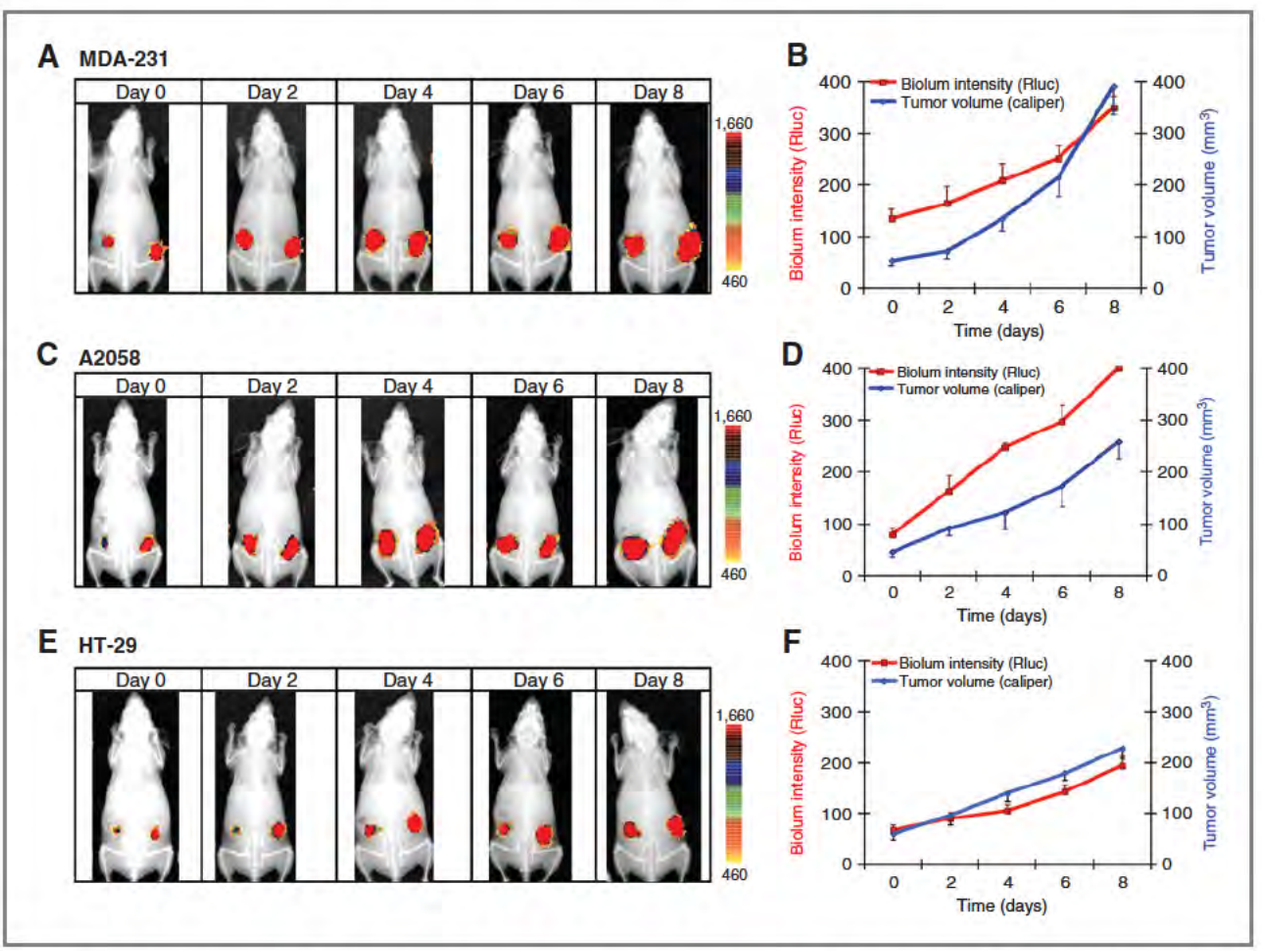

Figure 4. Tumor growth imaged with Rluc bioluminescence correlates with volumetric measurements obtained with caliper readings. The growth of human tumor xenografts imaged with Rluc bioluminescence. The Rluc signal areas in scans of bilateral MDA MB 231 Rluc flank tumors increased over time (A). The Rluc signal intensity increased and corresponded with caliper measured tumor volume (B). A similar expression was observed where the Rluc signal increase correlated with caliper measured tumor volume in A2058 Rluc (C, D) and HT29 Rluc (E, F) flank tumors. Data are expressed as the mean ± SEM.

Published OnlineFirst May 29, 2014; DOI: 10.1158/0008-5472.CAN-13-3472

of Rluc expression that defines tumor borders in the control group increased (Fig. 5A) whereas that in the virus treated group decreased over time (Fig. 5B). The corresponding cal culated Rluc signal intensities rose exponentially in the control group whereas it was markedly inhibited in the virus treated group ($P<0.004$; Fig. 5C). The decrease in reporter expression is suggestive of lytic replication. The caliper measured tumor volume showed a profile similar to Rluc measurements for the control group, but diverged for the treatment groups (Fig. 5D). This difference is attributable to the process that is measured in each case: Rluc defines a functional measurement that identifies viable cells, whereas caliper measurements are from external tumor diameters that also incorporate the necrotic tumor core (viable and nonviable tumor). The Fluc signal peaked 6 hours after virus injection and decreased over time (Fig. 5E). Quantified signal intensities revealed peaks every 2 days after the initial peak expression (Fig. 5F), which are indicative of newly released virions following a replication cycle as measured in plaque assays. Lytic replication reduces the number of viable cells for virus replication, which accounts for the decreasing Fluc signal. A similar response in virus and tumor dynamics was observed in the mouse colon cancer cell line (MC26 Rluc; Supplementary Fig. S2).

Dynamics of virus replication and tumor response to lytic replication imaged with PET

Virus replication in MC26 flank tumors was imaged with PET using [^{18}F]FHBG over 3 days after injecting 1×10^5 pfu hrR3 into the right flank tumor. Sites of virus replication were identified by intracellular phosphorylated [^{18}F]FHBG accumu lation. The intensity of the signal correlated with the magni tude of replicating virus (Fig. 6A). The control tumor had no [^{18}F]FHBG accumulation on PET. The time activity curves showed [^{18}F]FHBG accumulation in the virus infected tumor whereas the radiolabel was washed out of the control tumor, heart, and the liver (Fig. 6B). The fate of the cancer cells undergoing oncolysis was studied with [^{18}F]FLT PET imaging, which identified a highly proliferative tumor before virus injection. After virus injection, the signal decreased and the site of lytic replication was identified as central photopenia, which correlated with the area of tumor cell lysis (Fig. 6C).

Molecular PET and bioluminescence imaging data correlate with *in vitro* findings

Tumors that were imaged *in vivo* with bioluminescence and PET were excised to study growth characteristics before and after viral replication by immunohistochemical staining.

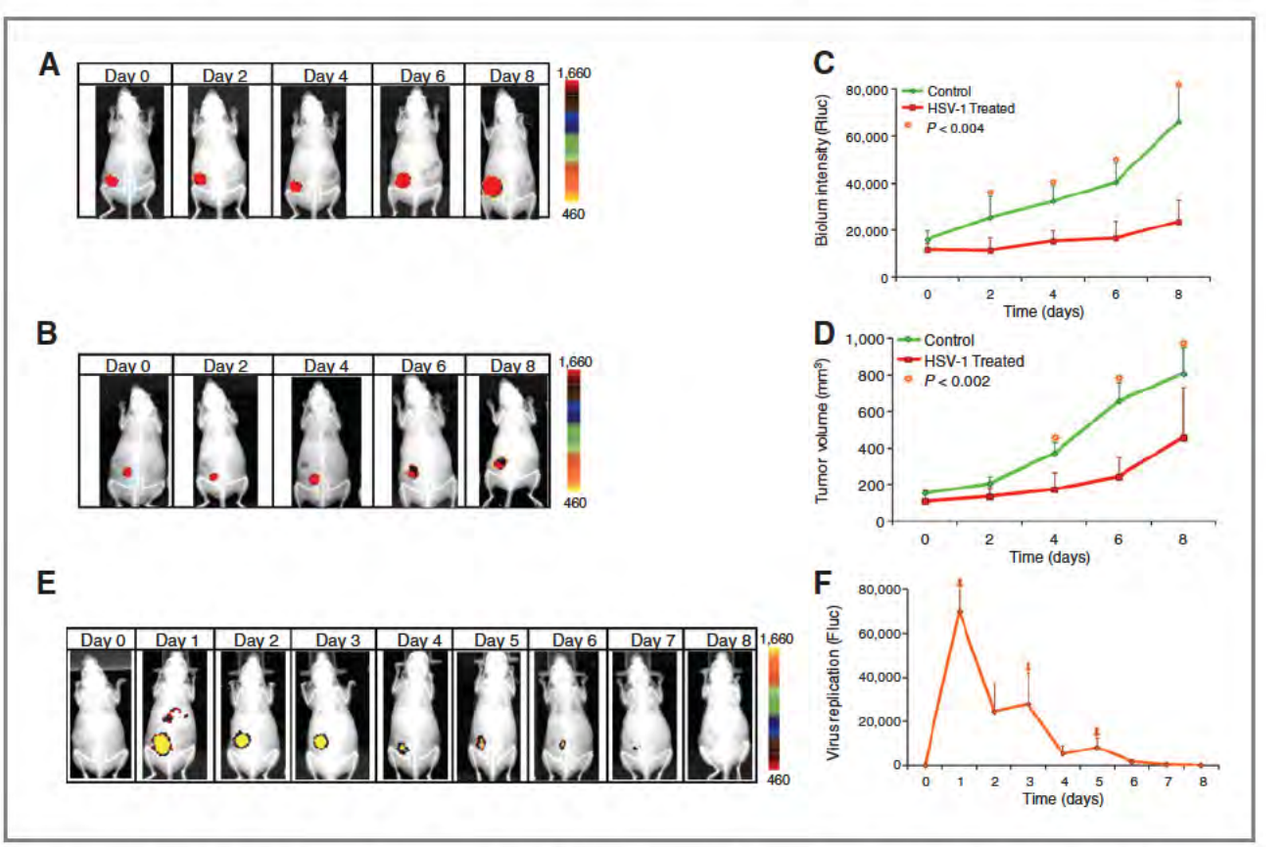

Figure 5. Tumor growth and viral replication kinetics imaged with dual bioluminescence. A, growth of MDA MB 231 Rluc flank tumors imaged with Rluc. B, growth inhibition of MDA MB 231 Rluc tumors undergoing viral oncolysis (1×10^8 pfu) imaged with Rluc. C, Rluc signal intensities in the control and virus treated groups. Rluc signal is shown as the mean net intensity/area ± SD. *, $P<0.004$. D, tumor volume measured with caliper readings in the control and virus treated groups. Tumor volume is shown as the mean ± SD. *, $P<0.002$. E, sequential imaging of virus replication with Fluc. F, the Fluc signal intensities peaked (arrows) several times as it decreased over time. Fluc signal is expressed as the mean net intensity/area ± SD.

Published OnlineFirst May 29, 2014; DOI: 10.1158/0008-5472.CAN-13-3472

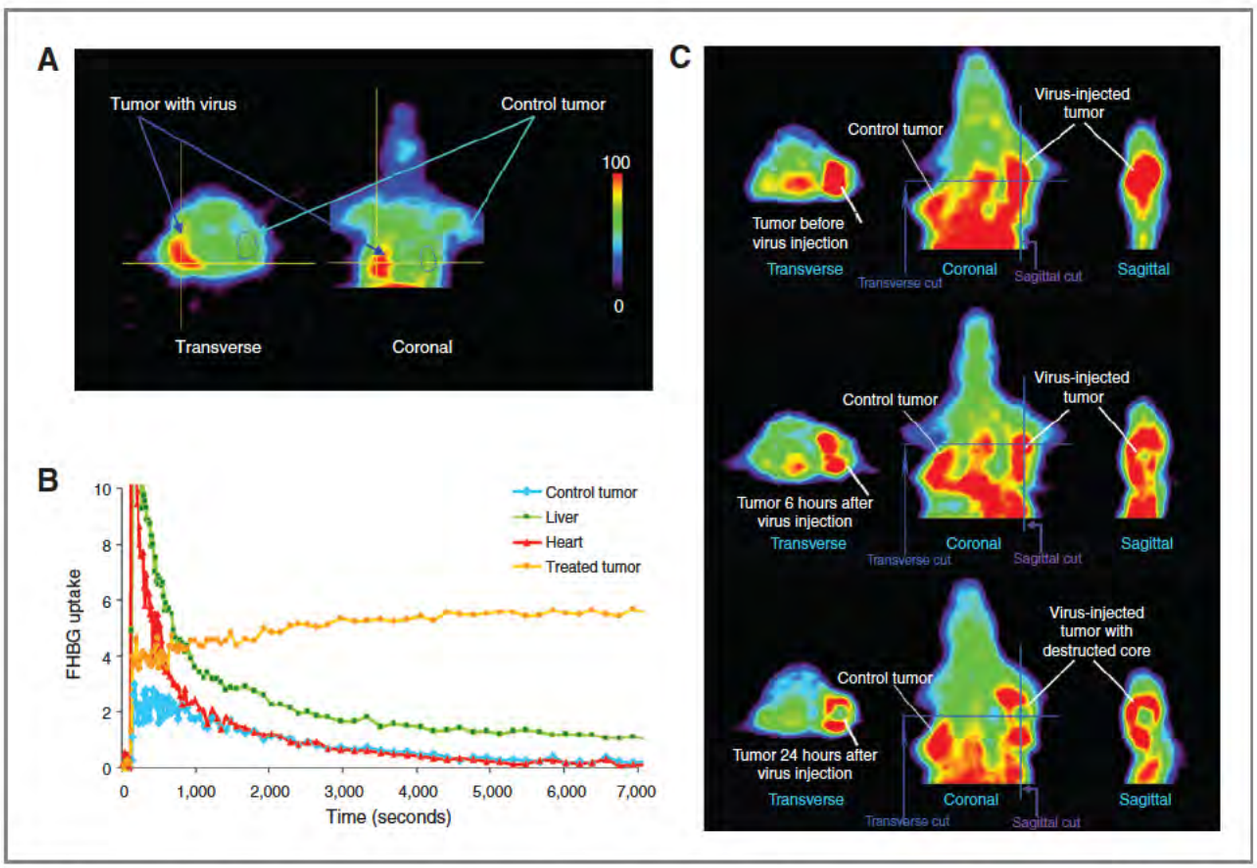

Figure 6. Dynamics of viral replication and cell proliferation imaged with microPET. A, localization of sites of virus replication in tumors with [^{18}F]FHBG PET. Virus was injected into the left of bilateral flank tumors. [^{18}F]FHBG uptake was seen in the virus infected tumor but not in the control tumor. B, time activity curves obtained from dynamic PET scans after [^{18}F]FHBG injection. [^{18}F]FHBG accumulated in the virus infected tumor, whereas it was washed off from the heart, liver, and control tumor. C, identification of proliferating tumor with [^{18}F]FLT PET. Photopenia identifies the site of virus replication in the tumor core.

Tumor cell proliferation imaged with [^{18}F]FLT PET, mCherry fluorescence, and Rluc bioluminescence correlated with PCNA immune staining of *ex vivo* tumor sections (Fig. 7A). Tumor destruction following virus replication was identified as a central loss of signal when imaged with Rluc bioluminescence, mCherry fluorescence, and [^{18}F]FLT PET. On *ex vivo* H&E staining, this central region was necrotic with a marked reduction in proliferating tumor cells (PCNA; Fig. 7B). Viral replication was identified with [^{18}F]FHBG PET and Fluc bio luminescence. Virus was detected with LacZ and HSV TK IHC on *ex vivo* tumor sections (Fig. 7B). The central core consisted of apoptotic cells.

Discussion

Successful treatment outcomes in preclinical animal models have set the stage for clinical trials of viral oncolysis as a novel cancer therapy (25). In these studies, the virus must be closely monitored to determine the accuracy of virus delivery to the tumor, as well as assessing viral titer locally and following viral replication at nontarget sites. Viral replication kinetics and biodistribution can be studied noninvasively by imaging virus gene expression that occurs intracellularly. Such information can be used to modulate virus dose, delivery routes, and the viral construct. In this study, we identified virus replication cycles as waves in the reporter gene expression in real time with bioluminescence and PET imaging. The peaks in these waves correspond to virions that are released at the end of a replication cycle. To our knowledge, this is the first report of sequential measurement of virus replication with biolumi nescence and PET, and the first to report on *in vivo* assess ment of intratumoral viral waves that provide continued tumor lysis after the initial wave of infection and oncolysis has occurred.

Bioluminescence is widely used in tumor biology to study growth characteristics and treatment response in cancers (26 29). In these models, bioluminescence reporters identify tumor growth, angiogenesis, and apoptosis in response to different treatments. And, bioluminescence studies have been con ducted for oncolytic vesicular stomatitis virus on prostate (26) and bladder cancers (30), oncolytic vaccinia virus on pancreatic (18), and oncolytic adenovirus therapy of gliomas (31) and ovarian cancer (32), as well as HSV 1 strains on hepatocellular carcinoma (HCC) (33). These studies limit their investigations to evaluating tumor response to lytic replica tion, without the study of viral replication itself. In addition, the

Published OnlineFirst May 29, 2014; DOI: 10.1158/0008-5472.CAN-13-3472

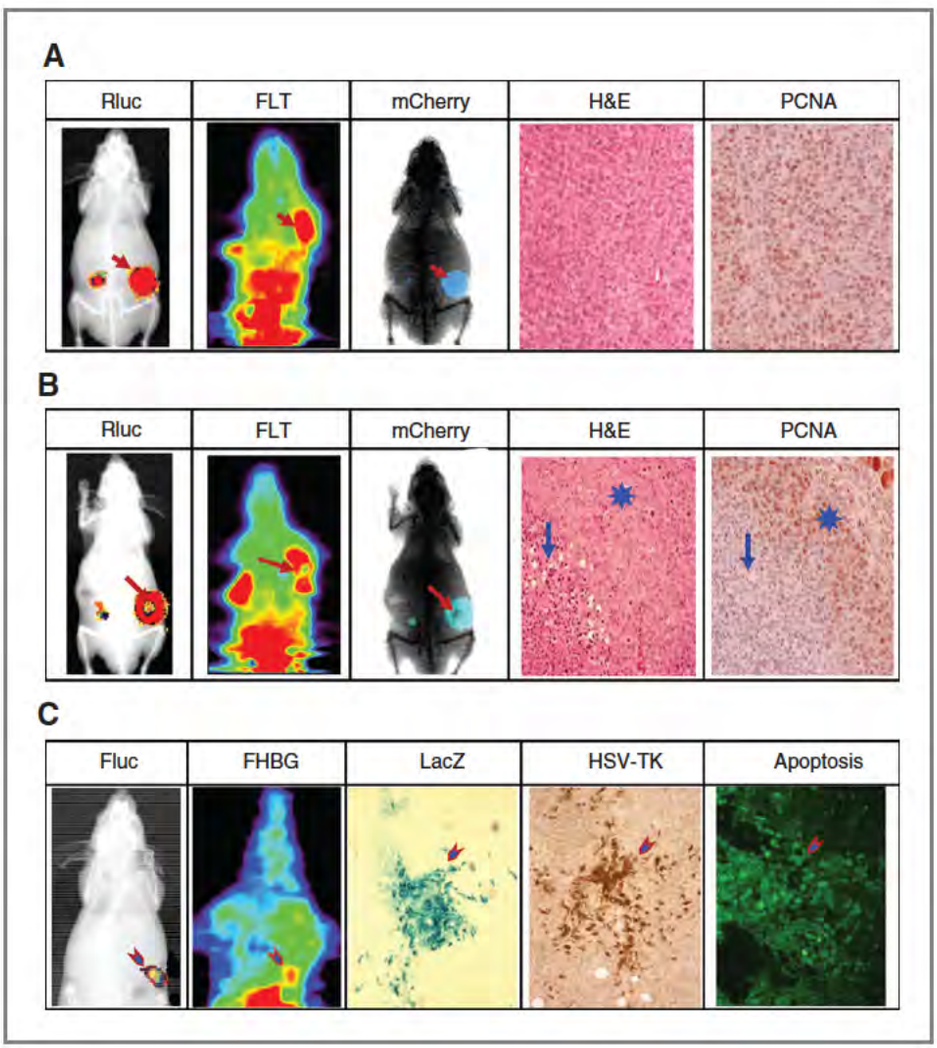

Figure 7. Correlation of bioluminescence, fluorescence, and microPET imaging data *in vitro*. A, tumor characteristics before virus administration. The tumor is identified with Rluc bioluminescence, mCherry fluorescence, and [^{18}F]FLT PET (small arrows). H&E and PCNA show highly proliferative tumors *in vitro*. B, changes in tumor characteristics following lytic virus replication. A destructed tumor core is identified with Rluc, mCherry, and [^{18}F]FLT PET (arrows), 48 hours after intratumor virus (1×10^8 pfu) injection. The changes are seen on H&E and PCNA where the destructed tumor core (arrow) is surrounded by a rim of viable tumor (asterisk). C, replicating virus is identified with Fluc bioluminescence and [^{18}F]FHBG PET. IHC staining for LacZ and HSV TK (arrow heads) in excised tumors confirm the presence of virus. Apoptosis is seen in the destructed tumor core.

properties of HSV 1, such as the infectivity of wild type virus in healthy mice (34), host immune responses to infection (35), transcriptional activity of early and late promoters (36), and the infectivity of various strains for cancer therapy (33) have been studied with bioluminescence. In these studies, virus was measured at a specific endpoint of the experiment. In contrast, we have dynamically studied HSV 1 replication and oncolysis with sequential imaging.

In most imaging studies involving HSV 1, the virus is used as an immunotherapy (e.g., T lymphocytes) for cancers (37) or as an amplicon to deliver cell based therapies (e.g., TNF related apoptosis inducing ligand; ref. 38). The TK gene of the virus is often used for prodrug activation with gancyclovir, or as the prototype PET reporter to image tumor growth and response to treatment. Most often the HSV TK gene is inserted into the genome of other oncolytic viruses to image those viruses with PET (17). However, the use of HSV TK to track the replication kinetics of its own virus, that of HSV 1, is limited. We previously demonstrated that HSV 1 oncolysis can be imaged with PET using the HSV TK as the reporter (21). In this study, we show that HSV 1 oncolysis and virus replication cycles can be studied with dual reporter imaging with bioluminescence and PET. We did not focus on imaging HSV 1 replication in metastases. However, in other studies, we have identified metastases at distant sites in the gut with bioluminescence and PET while imaging viral oncolysis treatment of liver metastases. With regard to immunity, we have previously reported no difference in antitumor activity of hrR3 in immu nocompetent and immunocompromised mice (22). The active immune system in immunocompetent mice neither enhanced nor attenuated antitumor effect of the virus.

We imaged two replication conditional HSV 1 viruses, HSV Luc and hrR3, with bioluminescence and PET. These mutants selectively replicate in proliferating tumors (10, 22, 23). We have analyzed tumor and normal liver parenchyma after hrR3 was injected into the spleen to deliver virus to treat liver metastases. No virus was detected in the normal liver. This observation has also been confirmed with *in vivo* imaging with bioluminescence and PET. Virus (hrR3 or HSV Luc) injected into a normal mouse (via the tail vein) was observed in the liver within 6 to 24 hours with a signal in the entire liver. This signal had completely resolved by 48 hours. However, in the case of a

Published OnlineFirst May 29, 2014; DOI: 10.1158/0008-5472.CAN-13-3472

mouse bearing liver metastases, virus was observed in the tumors beyond 48 hours whereas the signal had resolved in normal liver.

Out of the 2 replication conditional HSV 1 viruses used in this study, hrR3 is more robust and has a greater replication rate than HSV Luc, explaining the difference between the two initial imaging peaks for the viruses. The more robust hrR3 replication generated a replication peak at 6 hours instead of 24 hours as seen with HSV Luc. An additional contribution is likely related to different parent tumor lines undergoing ther apy in these studies. What is striking is that replication cycles can be monitored noninvasively with bioluminescence and PET, irrespective of the type of virus mutants or the type of cancer, suggesting the broad applicability of this approach to follow viral oncolysis *in vivo*, both preclinically and for clinical translation. The ability to assess oncolytic viral replication kinetics and spatial distribution *in vivo* has the potential to help optimize this therapeutic paradigm and accelerate clinical trials using targeted viral therapy.

Disclosure of Potential Conflicts of Interest

No potential conflicts of interest were disclosed.

Authors' Contributions

Conception and design: D. Kuruppu, U. Mahmood, K.K. Tanabe
Development of methodology: D. Kuruppu, A.-L. Brownell, U. Mahmood, K.K. Tanabe
Acquisition of data (provided animals, acquired and managed patients, provided facilities, etc.): D. Kuruppu, A.-L. Brownell
Analysis and interpretation of data (e.g., statistical analysis, biostatistics, computational analysis): D. Kuruppu, A.-L. Brownell, U. Mahmood, K.K. Tanabe
Writing, review, and/or revision of the manuscript: D. Kuruppu, A.-L. Brownell, K. Shah, K.K. Tanabe, U. Mahmood
Administrative, technical, or material support (i.e., reporting or organizing data, constructing databases): D. Kuruppu, K. Shah, K.K. Tanabe
Study supervision: A.-L. Brownell, U. Mahmood, K.K. Tanabe

Grant Support

This work was supported by NIH grants 5R01CA076183 and 5R21CA119600 (K.K. Tanabe), U01CA084301 and P50CA127003 (U. Mahmood), 5R01 EB001850, 1R01EB012864, and 1S10RR023452 (A.-L. Brownell), and Department of Defense (DOD) grant W81XWH-11-1-0388 (D. Kuruppu).

The costs of publication of this article were defrayed in part by the payment of page charges. This article must therefore be hereby marked *advertisement* in accordance with 18 U.S.C. Section 1734 solely to indicate this fact.

Received December 11, 2013; revised May 3, 2014; accepted May 20, 2014; published OnlineFirst May 29, 2014.

References

1. Roizman B. The function of herpes simplex virus genes: a primer for genetic engineering of novel vectors. Proc Natl Acad Sci U S A 1996;93:11307 12.
2. Martuza RL. Conditionally replicating herpes vectors for cancer ther apy. J Clin Invest 2000;105:841 6.
3. Mullen JT, Tanabe KK. Viral oncolysis. Oncologist 2002;7:106 19.
4. Chiocca EA. Oncolytic viruses. Nat Rev Cancer 2002;2:938 50.
5. Todo T. Armed oncolytic herpes simplex viruses for brain tumor therapy. Cell Adh Migr 2008;2:208 13.
6. Park K, Kim WJ, Cho YH, Lee YI, Lee H, Jeong S, et al. Cancer gene therapy using adeno associated virus vectors. Front Biosci 2008;13: 2653 9.
7. Coffey MC, Strong JE, Forsyth PA, Lee PW. Reovirus therapy of tumors with activated Ras pathway. Science 1998;282:1332 4.
8. Kuruppu D, Tanabe KK. Viral oncolysis by herpes simplex virus and other viruses. Cancer Biol Ther 2005;4:524 31.
9. Reinblatt M, Pin RH, Fong Y. Herpes viral oncolysis: a novel cancer therapy. J Am Coll Surg 2007;205:S69 75.
10. Goldstein DJ, Weller SK. Herpes simplex virus type 1 induced ribo nucleotide reductase activity is dispensable for virus growth and DNA synthesis: isolation and characterization of an ICP6 lacZ insertion mutant. J Virol 1988;62:196 205.
11. Kasuya H, Pawlik TM, Mullen JT, Donahue JM, Nakamura H, Chandrasekhar S, et al. Selectivity of an oncolytic herpes simplex virus for cells expressing the DF3/MUC1 antigen. Cancer Res 2004;64:2561 7.
12. El Deiry WS, Sigman CC, Kelloff GJ. Imaging and oncologic drug development. J Clin Oncol 2006;24:3261 73.
13. Bhaumik S, Gambhir SS. Optical imaging of Renilla luciferase reporter gene expression in living mice. Proc Natl Acad Sci U S A 2002;99:377 82.
14. Dothager RS, Flentie K, Moss B, Pan MH, Kesarwala A, Piwnica Worms D. Advances in bioluminescence imaging of live animal mod els. Curr Opin Biotechnol 2009;20:45 53.
15. Shah K, Weissleder R. Molecular optical imaging: applications leading to the development of present day therapeutics. NeuroRx 2005;2:215 25.
16. Luker KE, Luker GD. Bioluminescence imaging of reporter mice for studies of infection and inflammation. Antiviral Res 2010;86:93 100.
17. Ray P, Tsien R, Gambhir SS. Construction and validation of improved triple fusion reporter gene vectors for molecular imaging of living subjects. Cancer Res 2007;67:3085 93.
18. Haddad D, Chen CH, Carlin S, Silberhumer G, Chen NG, Zhang Q, et al. Imaging characteristics, tissue distribution, and spread of a novel oncolytic vaccinia virus carrying the human sodium iodide symporter. PLoS One 2012;7:e41647.
19. Tjuvajev JG, Doubrovin M, Akhurst T, Cai S, Balatoni J, Alauddin MM, et al. Comparison of radiolabeled nucleoside probes (FIAU, FHBG, and FHPG) for PET imaging of HSV1 tk gene expression. J Nucl Med 2002;43:1072 83.
20. Alauddin MM, Gelovani JG. Radiolabeled nucleoside analogues for PET imaging of HSV1 tk gene expression. Curr Top Med Chem 2010;10:1617 32.
21. Kuruppu D, Brownell AL, Zhu A, Yu M, Wang X, Kulu Y, et al. Positron emission tomography of herpes simplex virus 1 oncolysis. Cancer Res 2007;67:3295 300.
22. Yoon SS, Nakamura H, Carroll NM, Bode BP, Chiocca EA, Tanabe KK. An oncolytic herpes simplex virus type 1 selectively destroys diffuse liver metastases from colon carcinoma. FASEB J 2000;14: 301 11.
23. Kuroda T, Martuza RL, Todo T, Rabkin SD. Flip Flop HSV BAC: bacterial artificial chromosome based system for rapid generation of recombinant herpes simplex virus vectors using two independent site specific recombinases. BMC Biotechnol 2006;6:40.
24. Carroll NM, Chiocca EA, Takahashi K, Tanabe KK. Enhancement of gene therapy specificity for diffuse colon carcinoma liver metastases with recombinant herpes simplex virus. Ann Surg 1996;224:323 9.
25. ClinicalTrials.Gov Identifier: NCT01071941.
26. Moussavi M, Fazli L, Tearle H, Guo Y, Cox M, Bell J, et al. Oncolysis of prostate cancers induced by vesicular stomatitis virus in PTEN knock out mice. Cancer Res 2010;70:1367 76.
27. Sadikot RT, Blackwell TS. Bioluminescence imaging. Proc Am Thorac Soc 2005;2:537 40.
28. Serganova I, Moroz E, Vider J, Gogiberidze G, Moroz M, Pillarsetty N, et al. Multimodality imaging of TGFβ signaling in breast cancer metas tases. FASEB J 2009;23:2662 72.
29. Hawes JJ, Reilly KM. Bioluminescent approaches for measuring tumor growth in a mouse model of neurofibromatosis. Toxicol Pathol 2010;38:123 30.
30. Hadaschik BA, Zhang K, So AI, Fazli L, Jia W, Bell JC, et al. Oncolytic vesicular stomatitis viruses are potent agents for intravesical treatment of high risk bladder cancer. Cancer Res 2008;68:4506 10

Published OnlineFirst May 29, 2014; DOI: 10.1158/0008-5472.CAN-13-3472

31. Jang SJ, Kang JH, Kim KI, Lee TS, Lee YJ, Lee KC, et al. Application of bioluminescence imaging to therapeutic intervention of herpes simplex virus type 1 thymidine kinase/ganciclovir in glioma. Cancer Lett 2010;297:84–90.
32. Tsuruta Y, Pereboeva L, Breidenbach M, Rein DT, Wang M, Alvarez RD, et al. A fiber modified mesothelin promoter based conditionally replicating adenovirus for treatment of ovarian cancer. Clin Cancer Res 2008;14:3582–8.
33. Argnani R, Marconi P, Volpi I, Bolanos E, Carro E, Ried C, et al. Characterization of herpes simplex virus 1 strains as platforms for the development of oncolytic viruses against liver cancer. Liver Int 2011;31:1542–53.
34. Burgos JS, Guzman Sanchez F, Sastre I, Fillat C, Valdivieso F. Non invasive bioluminescence imaging for monitoring herpes simplex virus type 1 hematogenous infection. Microbes Infect 2006;8:1330–8.
35. Hwang S, Wu TT, Tong LM, Kim KS, Martinez Guzman D, Colantonio AD, et al. Persistent gammaherpesvirus replication and dynamic interaction with the host *in vivo*. J Virol 2008;82:12498–509.
36. Yamamoto S, Deckter LA, Kasai K, Chiocca EA, Saeki Y. Imaging immediate early and strict late promoter activity during oncolytic herpes simplex virus type 1 infection and replication in tumors. Gene Ther 2006;13:1731–6.
37. Dobrenkov K, Olszewska M, Likar Y, Shenker L, Gunset G, Cai S, et al. Monitoring the efficacy of adoptively transferred prostate cancer targeted human T lymphocytes with PET & bioluminescence imaging. J Nucl Med 2008;49:1162–70.
38. Shah K, Tang Y, Breakefield X, Weissleder R. Real time imaging of TRAIL induced apoptosis of glioma tumors *in vivo*. Oncogene 2003;22:6865–72.

Published OnlineFirst May 29, 2014; DOI: 10.1158/0008-5472.CAN-13-3472

Cancer Research
The Journal of Cancer Research (1916–1930) | The American Journal of Cancer (1931–1940)

AACR American Association for Cancer Research

Molecular Imaging with Bioluminescence and PET Reveals Viral Oncolysis Kinetics and Tumor Viability

Darshini Kuruppu, Anna-Liisa Brownell, Khalid Shah, et al.

Cancer Res 2014;74:4111-4121. Published OnlineFirst May 29, 2014.

Appendix B: SNMMI Poster

Characterization of a murine model of meningeal metastases from breast cancer

Darshini Kuruppu, Deepak Bhere, Chris Farrar, Anna-Liisa Brownell, Umar Mahmood, Misha Papisov, Kenneth Tanabe

Departments of Surgery and Radiology, Massachusetts General Hospital, Boston, MA 02114

Background

Meningeal metastasis is a fatal complication of breast cancer that affects 5-8% of patients when cancer cells seed in the meninges.

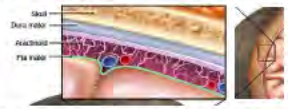

Subsequent growth of the cancer cells results in severe neurological complications involving the cranial nerves, cerebrum and spinal cord, limiting life expectancy to less than 4 months. Current treatment is largely palliative. Identifying disease progression will contribute to optimize therapeutic design and delivery.

Aim

To develop and characterize a model of meningeal metastases and characterize tumor progression with molecular MRI and bioluminescence imaging over time.

Methods

Meningeal metastases were created in nude balb/c mice using the MDA-MB-231 human breast cancer cell line that expresses Rluc. Tumor cells ($2x10^4$cells/10µl) were injected into the right lateral ventricle of the brain with stereotactic coordinates. Tumor growth in the meninges, brain and spinal cord was studied sequentially over 3 weeks with Gd-DTPA contrast T1 weighted 3D-MRI and Rluc bioluminescence imaging. Tumor volume was calculated from contrast uptake in MRI and Rluc signal intensities. The brains were studied *ex vivo* to confirm *in vivo* findings. The mice were observed for changes in body mass and external neurological symptoms.

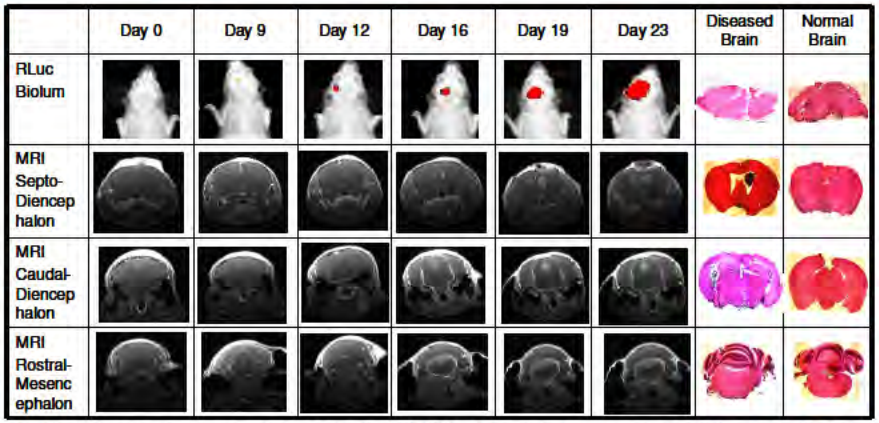

Fig 1: Serial imaging of meningeal metastases with Gd-DTPA-MRI and Rluc-bioluminescence. The Gd-DTPA contrast uptake in the brain regions are: **Septo-diencephalon:** contrast uptake seen initially in the right lateral ventricle migrates to the left lateral ventricle. **Caudal-diencephalon:** contrast visible in the 3rd ventricle and the inferior horn of the lateral ventricles. **Rostral-mesencephalon:** contrast seen in the optical track and the meningeal lining of the brain. **Rostral cerebellum:** contrast uptake in the 4th ventricle and in the base of the brain. Contrast uptake increases in intensity over time.

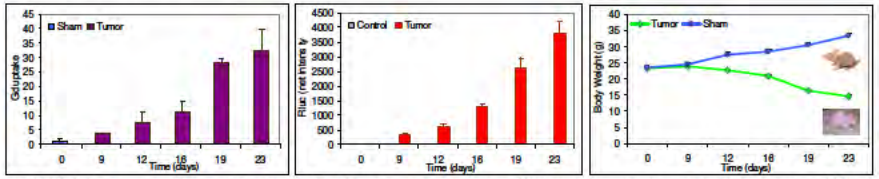

Fig 2: Defining tumor volume and body weight with meningeal metastases. 2A:The total tumor volume in the brain regions on MRI obtained with Gd uptake increases over time; 2B: Rluc signal increases over time tumor growth in the brain; 2C: As the tumors invaded the brain the diseased mice lose considerable weight compared to the controls.

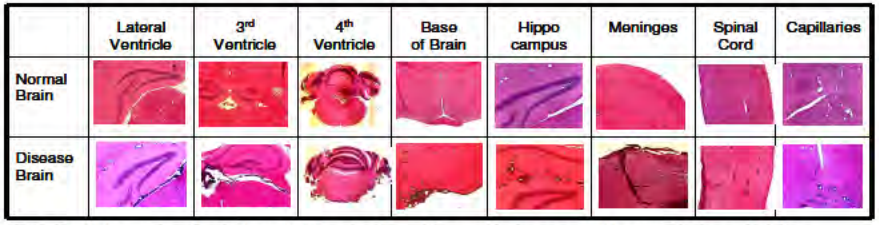

Fig 3: Identifying meningeal metastases in different regions of diseased brains compared to normal brains on histology.

Results

MRI identifies the anatomical location of the metastases. Disease progression is characterized by tumor invasion throughout the ventricular compartments and the meningeal lining of the brain. The latter stages are characterized with heavy tumor burden in the base of the brain that correlates with the severe neurological symptoms (bradykinasia, anorxia, and paralysis) in the mice. Tumor identified initially in right-lateral ventricle migrate to the left and inferior horns of the lateral ventricle, and the 3rd ventricle. Tumor is identified subsequently along the optical tracks, the 4th ventricle and the base of the brain. Histology reveals tumor aggregates in the thalamic region, hippocampus, and blood vessels of the *brain*, and along the lining of the *spinal cord* and its blood vessels. The expanding tumor volume is accompanied with a drastic reduction in body weight from emaciated body mass.

Discussion

We present a murine model of meningeal metastases with the sequential progression of disease characterized by molecular MRI and bioluminescence imaging, histology and change in body mass. The model resembles the human disease pathology and will serve as a platform to study novel treatments for meningeal metastases.

References

1. Chamberlain MC. Neoplastic meningitis. The oncologist 2008; 13; 967-977.

2. Clarke JL, Perez HR, et al. Leptomeningeal metastases in the MRI era. Neurology. 2010;74(18): 1449-54.

Funded by DOD

Appendix C: WMIC Oral Presentation

Kuruppu, Kumudu D.

From: adiaz@wmis.org
Sent: Thursday, June 19, 2014 11:58 AM
To: Kuruppu, Kumudu D.
Cc: Kuruppu, Kumudu D.
Subject: WMIC Abstract: Oral Presentation

Follow Up Flag: Flag for follow up
Flag Status: Flagged

Dear Darshini Kuruppu,

On behalf of the Program Committee, we are pleased to inform you that your abstract was selected for an Oral presentation at the World Molecular Imaging Congress. Each abstract was reviewed by five to ten peer reviewers in the abstract's specified field. The identity of the abstract submitter was protected to ensure scores were based on scientific merit.

Control ID: 1994387
Title: Novel oncolytic HSV-1 therapeutics for breast cancer meningeal metastases

We have copied your abstract's designated presenting author on this email. In the future, all communication will be with the presenting author.

If you are unable to present your work and need to withdraw your abstract, please email me by July 15, 2014. Withdrawals after this date may not be removed from conference materials.

If you have not already done so, it is very important that you register and book your hotel for the meeting to obtain the best rates. "Early Bird" registration ends July 9, 2014.

Registration: http://www.wmis.org/meetings/attending-the-conference/registration/

Reservations: http://www.wmis.org/book-your-hotel/

To create a personalized visa invitation letter: http://www.wmis.org/meetings/attending-the-conference/visa-information/

More details regarding specific date/time and preparation information for your presentation will be sent to the presenting author within two weeks. Congratulations and we look forward to seeing you in Seoul!

Kind regards,

Andrea Diaz
Program Manager
adiaz@wmis.org
P: 310.215.9730

Appendix D: SNMMI Abstract

Characterization of a murine model of meningeal metastases from breast cancer.

Darshini Kuruppu, Anna-Liisa Brownell, Kimmo Jokivarsi, Jacob Hooker, Umar Mahmood, Kenneth Tanabe

Background: Viral oncolysis by conditionally replicating Herpes simplex virus 1 (HSV-1) is a promising therapeutic option for cancers that are not responsive to current therapies, especially liver metastases. These viruses replicate in mitotically active cancer cells compared to quiescent cells. The resulting waves of virus replication following initial infection of a cell generate a maximal viral dose that is greater than the input dose. As such viral oncolysis therapy needs to be stringently monitored for the magnitude and sites of viral replication. At present this is achieved by tissue sampling (e.g. biopsy), a technique that is invasive and cumbersome for repetitive monitoring of virus in human subjects. A non-invasive molecular imaging technique such as PET can be manipulated to allow for localization of virus repetitively and quantitatively in real time. We present dynamic miroPET-CT imaging of HSV-1 mutant (HSV-Luc) in liver metastases following its administration via the portal circulation in a murine model using [18F]FHBG.

Methods: Focal liver metastases were created in balb/C mice by subcapsular insertion of tumor cells in matrigel. Virus (HSV-Luc at $1x10^7$ pfu) was administered into the spleen one week later when the tumors were approximately $10mm^3$. The conditionally replicating mutant HSV-Luc has the ribonucleotide reductase gene responsible for its replication inactivated by insertion of the β-galactosidase gene. HSV-Luc also expresses the firefly luciferase gene that allows for bioluminescence imaging with luciferin. HSV-1 expresses viral thymidine kinase, which allows for PET imaging with use of FHBG. The guanine derivative FHBG is phosphorylated by viral thymidine kinase which has a large substrate range compared to its mammalian counterpart, and phosphorylated [18F]FHBG is trapped intracellularly. Virus was imaged with PET at 3 and 5 days post virus administration using [18F]FHBG (100μCi). The tumors were subsequently resected to identify virus by LacZ staining.

Results: Bioluminescence detection of the virus with luciferin confirmed the expression of virus in the liver and tumors. PET-CT imaging at day 3 and 5 demonstrated virus in the focal liver metastases with PET two hours after [18F]FHBG injection by which time the radioligand is washed out from the liver. Time Activity Curves from the dynamic images confirmed the virus washout from the liver and accumulation in the tumor. Virus localized in the focal liver metastasis was clearly visible by PET imaging at both time points by 3D rendering. Virus in the tumor was visualized by in vitro staining for LacZ expression.

Conclusion: Virus expressed in focal liver metastases following its delivery into the portal circulation can be imaged non-invasively with PET using [18F]FHBG. This imaging capability allow for direct translation in to the clinics for determining sites and magnitude of viral replication in ongoing and future clinical trials of HSV-1 oncolysis for liver metastases.

Appendix E: WMIC Abstract

Novel oncolytic HSV-1 therapeutics for breast cancer meningeal metastases.

Darshini Kuruppu, Deepak Bhere, Chris Farrar, Khalid Shah, Aijun Zhu, KunEek Kill, Anna-Liisa Brownell, Umar Mahmood, Kenneth Tanabe.

Background: Meningeal metastasis is a fatal complication of breast cancer affects 5-8% of patients when circulating cancer cells seed in the meninges. Their subsequent growth causes severe neurological complications involving the cranial nerves, cerebrum and spinal cord, limiting life expectancy to less than 4 months. Currently there is no effective treatment, and aggressive multimodal therapies including intrathecal chemotherapy are often accompanied by severe toxicities. We have addressed this clear unmet need by investigating replication conditional HSV-1 oncolysis for meningeal metastases. Viral oncolysis is the destruction of cancer cells by replicating virus. Genetically engineered replication conditional HSV-1 mutants replicate preferentially in cancer cells rather than in normal cells. We present our findings in a well characterized murine model which resembles the human disease pathology.

Methods: Meningeal metastases were created in nude BALB/C mice using the MDA-MB-231 human breast cancer cell line that expresses Rluc. Guided by stereotactic coordinates, tumor cells were injected into the right lateral ventricle of the brain. Tumor growth in the meninges, brain and spinal cord has been studied in this model with sequential Gd-DTPA contrast T1 weighted 3D-MRI and Rluc bioluminescence imaging over 3 weeks. Oncolytic HSV-1 (HSV-Luc which expresses Fluc) was injected into the right lateral ventricle at 14 days. This time point resembles an intermediary disease phase after which tumors grow exponentially. Response by meningeal metastases to oncolytic HSV-1replication was imaged with MRI, and virus was imaged with [18F]FHBG-PET and Fluc bioluminescence. The brains were studied *ex vivo* to confirm *in vivo* findings. Tumor volume was calculated from MRI contrast uptake and Rluc signal intensities for treatment and control groups together with changes in body mass and external neurological symptoms.

Results: Oncolytic HSV-1 administration reduced meningeal metastases tumor burden in the disease mice. The reduction in tumor in the anatomical regions identified with Gd-MRI was seen primarily in the base of the brain and spinal cord. Virus replication at sites of proliferating tumor was identified with FHBG-PET imaging. Tumor and virus in the mouse brains was further confirmed with Rluc and Fluc bioluminescence imaging. Meningeal metastases were identified by histology with H&E and PCNA immunohistochemical (IHC) staining of the brains *ex vivo*. IHC staining for HSV-TK in these brains confirmed replicating virus in the meningeal metastases. Neurological symptoms (bradykinesia, ataxia, anorexia, and paralysis) that accompany a heavy tumor burden in the base of the brain were prevented in the animals that received virus. These mice gained weight compared to the control mice that became emaciated with considerable weight loss.

Conclusion: Replication conditional HSV-1 can be a novel treatment for breast cancer meningeal metastases. Based on our investigations oncolytic HSV-1 treatment at an intermediary phase of disease can inhibit life threatening disease progression. As such it holds promise as a potential therapy for breast cancer meningeal metastases.